FINAL TECHNICAL REPORT

NASA Research Grant NAG-1-279
University of Massachusetts Account # 5-28903
"Near Millimeter Wave Imaging/Multi-Beam Integrated Antennas"

IN-32
63709
42P

Period Covered:	1 June 1982 — 30 June 1986
Principal Investigator:	Professor K. Sigfrid Yngvesson
Co-Investigators:	Associate Professor Daniel H. Schaubert
	Asst. Prof. Karl D. Stephan
(The latter three	Asst. Prof. David M. Pozar
during earlier periods	Asst. Prof. T.C.L. Gerhard Sollner
of grant)	Asst. Prof. Peter T. Parrish

Department of Electrical and Computer Engineering
University of Massachusetts
Amherst, MA 01003

Table of Contents

1. INTRODUCTION

At the out–set of the grant effort being reported here, the plans were for pursuing work in three major areas: (1) Vivaldi/LTSA antenna elements (2) Microstrip Dipole and Patch Elements, and (3) A Demonstration system for Millimeter Wave Imaging Using an Array Feed. The work on Microstrip Dipole and Patch Elements was being performed primarily by Professor David M. Pozar, and was also supported by NASA Grant NAG–1–163. The final report for the latter grant, submitted in June 1984, summarized this entire effort, and we refer to that report for results in this area [1].

The remainder of the grant effort has been concerned with tasks (1) and (3) above.

Tapered slot antennas were first studied for use in phased arrays, and typically use a strip–line feed and are very short in order to be useable for wide–angle scanning. The term used for such antenna elements is the "notch" antenna [2]. There is a different category of applications for which a fairly narrow beam is required, in order to efficiently illuminate a focussing element such as a reflector or lens. Examples of such applications include multi–beam (switched or shaped) antennas for satellite communications, and multi–beam systems for imaging in connection with space science and remote sensing instruments. Tapered slot antennas can be designed to have narrow beamwidths and the first reported investigation which demonstrated the potential utility of tapered slot antennas for a number of such applications, was done by Gibson [3]. Gibson employed an exponentially tapered slot in the metalization on a dielectric substrate, and termed this antenna element the "Vivaldi" antenna. He showed that the Vivaldi antenna can be designed such that the beamwidth is approximately constant over a frequency band of several octaves, provided that the exponential opens up sufficiently rapidly. The study performed under this grant has primarily dealt with linearly tapered slot antennas (LTSA's) and constant width slot antennas (CWSA's), see Figure 1. Instead of emphasizing the constant beam–width versus frequency, we have studied how the shape, dielectric thickness, and antenna length influence the beam–shape and beam–width of more gradually tapered slot antennas than those of Gibson in order to make a contribution toward the understanding of their radiation mechanism as well as to make available design information. We have also developed

design information for arrays of LTSA elements, and demonstrated a prototype 94 GHz multi-beam system using an LTSA array in a Cassegrain reflector.

2. SINGLE ELEMENTS OF TAPERED SLOT ANTENNAS

A. *Experimental Results and Semi-Empirical Models*

A.1. Beam-Shape and Beam-Widths

Early studies of linearly tapered slot antennas (LTSA's) under this grant showed that acceptable beam-shapes could be obtained over a wide range of antenna lengths, i.e. about 3 to 15 free space wavelengths. The beamwidths were narrower than those of other integrated circuit antennas, such as microstrip dipoles and patches, for this range of antenna lengths, and one of our aims was to identify design methods which would lead to elements which could illuminate practical reflector antennas. A typical optimum taper at the reflector edge is -10 dB, and it was shown that tapered slot antennas could be designed with the -10 dB beamwidth down to about 25-30 degrees, corresponding to a value of f/D of about 2. Problems were encountered with thick dielectric substrates, however, especially for long antennas. In an extreme case, the beam would develop a null on axis. It was known that many of the same features, such as the decreasing beamwidth for increasing antenna length, and the sensitivity to too much dielectric slowing, had been noticed in the general class of antennas called traveling-wave antennas. These have been reviewed in detail by Zucker [4]. The empirical studies showed that Zucker's standard data for traveling-wave antennas were a good design guide for LTSA's, provided that the antenna parameters were within a range, which is specified below:

(1) The opening angle should be close to 11 degrees for the beamwidths in the E- and H-planes to be approximately equal (the fact that this is possible is one of the most notable advantages of tapered slot antennas),

(2) The width of the metalization outside the slot should be at least 2-3 wavelengths, otherwise there is a beamwidth dependence upon this parameter, see section B below.

(3) The effective dielectric thickness, defined in the equation below, should be in the range 0.005 to 0.01 wavelengths:

$$\frac{t_{eff}}{\lambda_o} = \frac{t(\sqrt{\epsilon_r} - 1)}{\lambda_o} \qquad (1)$$

With the effective dielectric thickness in this range, LTSA's will give beamwidths generally within the limits for standard traveling–wave antennas, given by Zucker. A thicker substrate leads to a narrower beam–width, closer to the curve designated "high gain" by Zucker. If the substrate thickness is increased further, then the beam shape will generally experience fairly drastic changes. An example of the effect of substrate thickness is shown in Figure 2 which compares beamwidths for three different thicknesses of Kapton with standard traveling–wave antenna data. Other examples are given in the publications {1} and {6}. (Note: References cited with these brackets ({}), are to be found in Section 5 of this report – the itemized list of all publications based on this grant, other references are cited with a square bracket, and given in section 6). LTSA's with air dielectric also work well in general, but have wider beams than the standard traveling–wave antennas.

A.2. Directivity and Beam–Efficiency

The directivity of an LTSA element generally increases with its length, as shown in Figure 3. In many early measurements, the directivity fell below the range indicated by Zucker for standard traveling–wave antennas, or close to the "low–sidelobe" curve. This fact indicates that the side–lobe levels can be rather high. In some cases, the side–lobe level was not measured correctly because the signal–to–noise ratio was not sufficient. This applies especially to measurements at 94 GHz. Nevertheless, the values obtained for directivity were the highest for any integrated circuit antenna, up to about 17 dB for the longest elements. Beam efficiencies at the –10 dB level were typically about 30% for antenna elements 10 wavelengths long, and 40–50% for somewhat shorter antennas. Both directivities and beam–efficiencies have steadily improved, as the grant effort proceeded, and more was learned about how to achieve low side–lobes. Present values result in directivities up to 20 dB, and beam–efficiencies up to 70–80%. These new data will be reported in detail in the first report for the new contract with Langley Research Center.

A.3. Impedance

The input impedance has been calculated based on conformal mapping, and agrees well with measurements, as shown in Figure 4. The impedance is independent of frequency over a range of several decades.

B. *Theoretical Results and Models*

B.1. Theoretical Approach

A number of initial theoretical approaches gave useful but not very accurate results. The approach which was subsequently used is successful in predicting beamwidths and central beamshapes very accurately, and sidelobe–levels and side–lobe positions with good accuracy (for details, see the Ph.D. thesis of R. Janaswamy, included with this report as Appendix A). The parameters of antenna length, taper shape, and dielectric substrate permittivity and thickness were varied. Two different models were used:

(1) For air dielectric LTSA elements, it is possible to use a bi–fin model (see Figure 5), which allows a TEM– mode solution for the fields along the structure. The field distribution along a finite length slot was then used for an aperture integration, which resulted in the far–field radiation pattern. The theoretical and experimental patterns agree well and are compared in Figure 6.

(2) In the second approach, used for more general shapes, and for dielectric–supported antennas, the solution proceeds in two steps. The geometry for the general approach, is illustrated in Figure 7.

The method of analysis consists of two steps. In the first step, the tangential component of the electric-field distribution in the tapered slot, hereafter referred to as the aperture distribution, is obtained. In the second step, far-fields radiated by the equivalent magnetic current in the slot are obtained by using an appropriate Green's function.

The aperture distribution in the tapered slot is determined by employing the usual travelling wave antenna assumption that the aperture distribution is governed predominantly by the propagating modes corresponding to the non-terminated structure. The effect of the termination of the structure at ABCD can be incorporated by adding a backward travelling wave. One recognizes that under these conditions, the problem reduces to finding the field distribution for the case of a tapered *slot line*. To accomplish this, the continuous taper is approximated by means of a number of sections of line of uniform width connected end to end. This is illustrated in Fig. 7B. The slot wavelength and the characteristic impedance vary from section to section in accordance with the slot width. At this stage, one may use the theory of small reflections [5] to get an estimate for the overall

reflection coefficient arising from reflections from each of the step junctions and from the termination. However, for a long travelling wave antenna, the backward travelling wave on the structure does not contribute much to the front lobe. Numerical studies have shown that the contribution due to the backward wave can be ignored whenever $L \geq 3\lambda_o$.

The aperture distribution for the stepped model is found in the following manner. Solution to the eigenvalue problem for a uniform slot line completely determines the aperture distribution in each parallel section (the slot electric field is determined up to a multiplicative constant and this is of no consequence if one were interested in a uniform slot line alone). To account for the step discontinuity, a power continuity criterion (i.e., constant power flow along the axis of the tapered line) is enforced at the step junction. This criterion relates the undetermined multiplicative constants in each section, thus yielding the field distribution in the stepped structure corresponding to a forward travelling wave on the aperture. Data on the characteristic impedance of a wide uniform slot line are needed to enforce this criterion. The slot wavelength, the slot electric field and the characteristic impedance of a uniform wide slot line on a low permittivity substrate are obtained in {5}, and {7}.

The second step in the analysis is the determination of the fields radiated by the tapered slot using the field distribution found in the first step. Termination of the aperture results in the edge ABCD in the metalization, and currents are induced due to edge diffraction. These must be included in the analysis. The edge induced currents are important because the radiation pattern of a slot in an infinite ground plane (i.e., without taking the edge ABCD into account) has a null in the plane of the conductor. The prospective Green's function must be able to directly accommodate this important phenomenon. It is seen from Fig. 7 that the slot extends as far as the edge ABCD, thus precluding the use of far-field ray scattering theories such as GTD and UAT. This important near-field scattering is taken into account by treating the slot as radiating in the presence of a conducting half-plane (i.e.,the half-plane Green's function is used).

It may also be noted that a simple analysis based on approximating the currents on the metalization as flowing along wires—similar to a V-antenna—and subsequently using the free space Green's function to find the far-fields is not satisfactory. Such a model

incorrectly predicts a minimum in the end-fire direction as the flare angle $2\gamma \rightarrow 0$ (as in a CWSA), whereas the two step procedure described above correctly predicts an end-fire main beam. The success of the latter is attributed mainly to the use of the half-plane Green's function.

Tai [6] has developed the exact theory of infinitesimal slots (both—one sided and two sided) radiating in the presence of a conducting half-plane . This half-plane Green's function is used in conjunction with the aperture distribution found in step one to compute the far-fields radiated by each uniform section. Radiation from the entire length is determined by adding the contributions from all the sections.

B.2. **Interpretation of Results**

Most of the features of the radiation pattern of LTSA antennas, with or without dielectric, can be discussed in terms of the behavior of the TEM model.

(1) Dependence of Beamwidth on Flare Angle (2γ).

The beamwidth in the H–plane is independent of the flare angle for a constant antenna length, L, and decreases with the flare angle in the E–plane, but not as fast as inversely proportional to the angle (see Figure 8).

(2) Dependence of Beamwidth on Antenna Length, L.

The 3 dB beamwidth in the H–plane depends on antenna length exactly as predicted for a traveling–wave antenna model, assuming a phase–velocity equal to the vacuum speed of light (see Figure 9). In the E–plane, a somewhat more rapid dependence on L is seen, see Figure 10.

The conclusion from these data is that the TEM LTSA antenna behaves as a traveling–wave antenna as far as its H–plane radiation pattern is concerned. The E–plane beamwidth behaves somewhere in between that of a pure traveling–wave antenna and an aperture antenna. For example, the dependence of E–plane beamwidth on normalized length, would be roughly inversely proportional to the angle (for small angles), if the beamwidth were determined by the size of the aperture at the edge. The beamwidth in the E–plane varies more slowly than this. Also note that for constant length, the H–plane beamwidth is independent of flare angle, as expected, whereas the E–plane beam width depends on flare angle, but not as rapidly as predicted for an aperture antenna.

The general features of the radiation patterns for TEM antennas, which we discussed in the previous paragraph, are still present for dielectric–supported antennas, with modifications which can be traced to the lower phase–velocity. The beamwidths, beam shapes, and sidelobe levels generally show good agreement between experiment and theory as shown for an LTSA on thin dielectric in Table 1. For thin dielectrics, a correction of –2.5% is required to the phase velocity, compared with the theoretical value for a wide slot. For thick, or high dielectric constant, substrates, this correction is not needed. This is a question which will require some further exploration. Another so far unsolved problem is that of the LTSA with a finite width strip outside the slot. As mentioned above in section A, the beamwidth depends on this dimension. Theoretical efforts for this geometry have not yet been successful.

(3) Dependence of Beamshape on Shape of the Tapered Slot

The stepped taper model can also be used for other shapes than the LTSA with good agreement. In Figures 11 through 13, we show calculated beamshapes for CWSA, LTSA and Vivaldi elements of the same length and on the same substrate. Note the lowering of the sidelobe level in the H–plane, as the shape becomes more gradually tapered, in going from the CWSA through the LTSA to the Vivaldi.

3. A PROTOTYPE IMAGING SYSTEM USING A SEVEN ELEMENT LTSA ARRAY

Much of the interst in tapered slot radiating elements is connected with the ability to construct integrated, low–cost arrays. In order to clearly demonstrate the feasibility of such arrays in an actual operating system, we have investigated rather thoroughly a millimeter–wave (94 GHz) prototype seven–beam system, using a one–foot diameter Cassegrain reflector antenna. The array thus was designed to match the optics of this reflector, which was a standard design often used in millimeter wave applications and commercially available. The sub–reflector is seen under an angle of 30 degrees from the final focus, which is located a small distance in front of the main dish. The arrangement is illustrated in Figure 14. A seven–element array as shown in Figure 15 was developed.

The first step in the development was to design a single element which had the desired beamwidth of about 30 degrees in both major planes at the –10 dB level. Modeling at X–band frequencies showed that an LTSA on a thin dielectric (6 mil Duroid was used) would match these specifications if it had an electrical length of about 10 wavelengths. Since 6 mil is the thinnest Duroid available, it was necessary to choose a different dielectric material for 94 GHz. One mil Kapton turned out to result in an element at this frequency which has a symmetric beam see Figure 16. By choosing a length which does not strictly scale with the frequency–ratio, we were thus able to meet our specifications. This element was demonstrated at the presentation our group gave at NASA Langley Research Center in September, 1982.

An LTSA array with an element spacing of about 2.5 wavelengths was first tested by modeling at X–band, and it was quickly found that the individual beams of the elements in this array were very similar to that of a single element. The same applies to arrays on Kapton, used at 94 GHz. The seven element array was measured in the Cassegrain antenna in a test range, shown schematically in Figure 17. The length of the range was 50 meters, and the data should therefore be representative of far–field data to a good accuracy. A Gunn oscillator source was used as the transmitter, and the detected signals from diodes soldered at the narrow end of each LTSA were measured as the dish scanned the source in either the E–plane or the H–plane. Representative scans are shown in Figure 18. Elements off the axis show expected phenomena such as a coma side–lobe, but all element positions in the array produce beams which are very well useable. This system was demonstrated at the site visit by NASA Langley personnel in September, 1983. Subsequent measurements explored even smaller separation between the elements of the array than the original 7.9 mm, i.e. 5 and 3 mm, respectively. Element patterns (i.e. without the dish) with a 5 mm spacing show a narrowing of the E–plane pattern and a widening of the H–plane pattern. Despite the changed beam–shape, the spill–over beam–efficiency is actually slightly better than for the 7.9 mm spacing (35 versus 31%). The beam–spacing, however, is almost the same in the two arrays, i.e. somewhat less than a beamwidth, with a corresponding cross–over level for adjacent beams of about –2 dB. The seven–beam Cassegrain system

was described in a paper given at the Eighth IEEE International Conference on Infrared and Millimeter Waves in 1983 {15}.

More recently, a similar array consisting of 25 (5×5) CWSA elements, was used in a one–foot diameter prime–focus paraboloid at 31 GHz. This system had a smaller f/D of 1.0, and showed a higher beam efficiency of about 65%. The beam spacing achieved was about one beamwidth. This system has been reported at the SPIE Conference on Submillimeter Spectroscopy in Cannes, France, in Dec. 1985, as well as at the Tenth International Conference on Infrared and Millimeter Waves, also in December, 1985 {16, 17}.

It is very important for the practical utilization of LTSA arrays to note that the closest spacing between circular waveguides used in the same system is 14 mm, with a beam spacing of about two beamwidths. This is one of the most interesting properties of the LTSA array. There are other ways to illustrate the uniqueness of the LTSA array in this respect. We have for example used a plot from a paper by Rahmat–Samii et al [7] to compare LTSA elements with other elements such as the CWSA elements mentioned above, rectangular and circular waveguides, a pyramidal horn, and the cigar antenna. If one approximates the beam pattern of these elements with a $(\cos\theta)^q$ shape and plots the value of q as a function of the array spacing, d, normalized with respect to wavelength, then one obtains a plot such as shown in Figure 19. The q–value for the LTSA array is more than a factor of 2 higher than for any other element at the spacing where we measured it. One notes that the cigar antenna, which has the highest q of the other elements, also makes use of a traveling wave radiation process.

In terms of another parameter, we can also investigate the properties of the LTSA array as used in a multi–beam system by finding how closely it approaches the so–called diffraction–limited resolution, as given by the following expression, if the radiation sampled is incoherent:

$$T_I = (\lambda/2) \star f\#$$

Here, $f\#$ is the f–number of the optics used and is equal to 1.9 in our prototype system. At a wavelength of 3.19 mm, then, we find that $T_I = 3.0mm$. We can also estimate that this spacing corresponds to about 0.42 beam–widths of the system, in agreement with

the sometimes quoted requirement to sample twice per beamwidth in order to achieve diffraction–limited resolution. The minimum beam spacing achieved in our prototype system is 0.5° with a measured 3 dB beamwidth (average between E– and H–planes) of 0.7°. The beam spacing is thus close to 0.7 of a beamwidth, or a little less than a factor of two times the diffraction–limited resolution spacing.

In view of the high packing density which has been demonstrated for LTSA arrays, it has been of interest to study the inter–element coupling. We mentioned above that the beam–shapes of individual elements were affected by coupling in the 5 mm spacing array but not the 7.9 mm spacing array. Recently, we have explored this further in a 3 mm spacing array. This extremely densely packed array yields beams which tend toward omni–directional if more than one substrate is used. For the one substrate case, however, a main beam results, which has somewhat lower beam efficiency (15–20%), than for the larger spacings. Also, for a substrate with three elements, one finds that the directions of the individual beams have been shifted quite noticeably. While for 5 and 7.9 mm spacing arrays, one cannot detect any changes in the radiation pattern of a particular element with the other elements are either shorted or left open–circuited, quite large effects are seen for the 3 mm spacing array. Figures 20 and 21 show some examples of this effect. It is clear that such results can yield information which gives clues to the theoretical model for LTSA arrays, which remains to be explored in detail.

4. REVIEW OF INTEGRATED LTSA WITH RECEIVER ELEMENTS RESULTS

We have obtained and published some preliminary results on a mixer design which is suitable for integration with tapered slot antennas {18}. This mixer design was tested both in a 4–10 GHz model, and (slightly modified) at 94 GHz. The 94 GHz mixer utilized the same Hewlett–Packard beam–lead diodes which we used as detector diodes in the LTSA arrays. These diodes are the most rugged which we have found, and generally survive well on the flexible kapton substrates. The 4–10 GHz version of this mixer has less than 6 dB conversion loss over an octave bandwidth. It uses a slot–ring in a balanced configuration, and requires the LO to be fed through a separate port.

A different design for a mixer which may be integrated with an LTSA antenna element is shown in Figure 22. This mixer was tested at 38 GHz with the same HP beam–lead diodes, and has less than 10 dB conversion loss. In this case, both signal and LO are coupled through the same port, which is convenient in many cases. One should note that the HP diodes are intended for use up to 18 GHz, and that consequently the conversion loss at 38 GHz is expected to be somewhat high.

Further work on mixers has emphasized theoretical modeling, using a computer program originated by Dr. A. Kerr and others at the Goddard Institute for Space Studies, New York, N.Y. The program was expanded to take into account the effect of excess noise in Schottky–barrier diodes for the first time. Calculated results agree qualitatively with measured results on millimeter wave mixers, see {2}, {9}, and {20, 21}. This work was partially supported on the grant.

5. PUBLICATIONS BASED ON WORK ON THE GRANT

5.A. *Ph.D. Theses Based on Work on the Grant.*

1. Korzeniowski, T.L., "A 94 GHz Imaging Array Using Slot Line Radiators", September 1985.
2. Hegazi, G.M., "Optimization of Low-Noise Millimeter Wave Receiver Front-Ends", May 1986 (partially supported by the grant).
3. Janaswamy, R. "Radiation Pattern Analysis of the Tapered Slot Antenna", August 1986.

5.B. *Chapters in Books*

4. Yngvesson, K.S. "Near-Millimeter Imaging with Integrated Planar-Receptors: General Requirements and Constraints", Chapter 2 of Volume 10, Infrared and Millimeter Waves (K. Button, Editor), Academic Press, 1983.

5.C. *Papers in Journals*

5. Janaswamy, R., and Schaubert, D.H., "Dispersion Characteristics for Wide Slotlines on Low-Permittivity Substrates", IEEE Trans. Microw. Theory Techn., MTT-23, 723—726 (Aug. 1985).
6. Yngvesson, K.S., Schaubert, D.H., Korzeniowski, T.L., Kollberg, E.L., Thungren, T., and Johansson J., "Endfire Tapered Slot Antennas on Dielectric Substrates", IEEE Trans. Antennas and Propagat., AP-33, 1392—1400 (1985).
7. Janaswamy, R., and Schaubert, D.H., "Characteristic Impedance of a Wide Slot Line on Low Permittivity Substrates", IEEE Trans. Microw. Theory Techn., MTT-34, 900—902 (Aug. 1986).
8. Janaswamy, R., Schaubert, D.H., and Pozar, D.M., "Analysis of the TEM Mode Linearly Tapered Slot Antenna", to appear in Radio Science.
9. Hegazi, G.M., Jelenski, A., and Yngvesson, K.S., "Limitations of Microwave and Millimeter Wave Mixers Due to Excess Noise", IEEE Trans. Microw. Theory Techn., MTT-33, 1404—1409 (Dec. 1985). (Partially supported)
10. K.S. Yngvesson, J.F. Johansson, and E.L. Kollberg, "A New Integrated Slot Element Array for Multi-Beam Systems", to appear in IEEE Trans. Antennas and Propagat., AP-34 (November, 1986).

5.D. *Papers Given at Conferences*

11. Kollberg, E.L., Thungren, T., and Yngvesson, K.S., "Vivaldi Antenna/Fin-Line Circuit for SIS Mixers", 6th Int. Conf. Infr. Millimeter Waves (1981).
12. Thungren, T., Kollberg, E.L., and Yngvesson, K.S., (1982). 12th Eur. Microw. Conf. p. 361.
13. Kollberg, E.L., Johansson, J.F., Thungren, T., Korzeniowski, T.L., and Yngvesson, K.S., "New Results on Tapered Slot Endfire Antennas on Dielectric Substrates",

Eighth IEEE International Conference on Infrared and Millimeter Waves, Miami, Fla., Dec. 1983.

14. Korzeniowski, T.L., Pozar, D.M., Schaubert, D.H., and Yngvesson, K.S., "Imaging System at 94 GHz Using Tapered Slot Antenna Elements", IEEE International Conference on Infrared and Millimeter Waves, Miami, Fla., December 1983.

15. Johansson, J., Kollberg, E.L., and Yngvesson, K.S., "Model Experiments with Slot Antenna Arrays for Imaging", SPIE Conference on Millimeter Wave Imaging, Cannes, France, Dec. 1985.

16. Schaubert, D.H., and Yngvesson, K.S., "Near Millimeter Imaging Techniques Using Integrated Planar Feed Arrays", Tutorial Talk at URSI General Assembly, Commission J, Florence, Italy, Aug. 1984.

17. Yngvesson, K.S., Johansson, J., and Kollberg, E.L., "Millimeter Wave Imaging with an Endfire Receptor Array", 10th International Conference on Infrared and Millimeter Waves, Orlando, Fla., Dec. 1985.

18. Cai, S.Z., and Yngvesson, K.S., "Broadband Slot–Ring Balanced Mixer for Millimeter Waves", Eighth International Conference on Infrared and Millimeter Waves, Miami, Fla., Dec. 1983.

19. Yngvesson, K.S., "Imaging Front–End Systems for Millimeter WAves and Submillimeter Waves", in SPIE Proceedings, Volume 598, 104—113 (Dec. 1985). "Instrumentation for Submillimeter Spectroscopy".

20. Hegazi, G.H., Jelenski, A., and Yngvesson, K.S., "Limitations of Microwave and Millimeter Wave Mixers Due to Excess Noise, IEEE MTT-S International Microwave Symposium, 1985 (partially supported).

21. Hegazi, G.H., Jelenski, A., and Yngvesson, K.S., "Design of Low Noise Millimeter Wave Mixers Taking into Account Excess Noise in the Diode," 10th International Conf. Infrared Millimeter Waves, Dec. 1985.

22. Janaswamy, R., and Schaubert, D.H., "Analysis of the Tapered Slot Antenna", IEEE AP–S Symposium Digest, Vol. 2, pp. 689—692, Philadelphia, PA, June 1986.

23. Yngvesson, K.S., Johansson, J.F., and Kollberg, E.L., "A New Integrated Array for Multi–Beam Systems with Application to Millimeter Imaging", ibid, pp. 895—898.

24. Winkler, D., McGrath, W.R., Nilsson, B., Claesson, T., Johansson, J.F., Kollberg, E.L. and Rudmer, S., "On the Feasibility of Constructing an Imaging Array of Slot–Antennas Integrated with SIS Mixers", Proceedings of the ESA Workshop on the FIRST (Far Infrared and Submillimeter Wave Space Telescope), Segovia, Spain, June 1986, 7 pages.

6. REFERENCES

1. Pozar, D.M., "Analysis of Microstrip Antennas", Final Report TR-28912, NASA LaRC Grant NAG-1-163, June 1984.
2. Lewis, L.R., Fassett, M., and Hunt, J., "A Broadband Stripline Array Element", IEEE AP-S Symposium, June 1974, p. 335.
3. Gibson, P.J., (1979), 9th Eur. Microw. Conf., Brighton, U.K., 101—105.
4. Zucker, F.J., "Surface- and Leaky-Wave Antennas", in **Antenna Engineering Handbook**, H. Jasik, Ed., McGraw-Hill, New York, (1961), pp. 14—16.
5. Collin, R.E., *Foundations for Microwave Engineering*, Chap. 5, McGraw Hill, New York, 1966.
6. Tai, C.T., *Dyadic Green's Functions in Electromagnetic Theory*, Inter. Educational Publishers, Scranton, PA, 1971.
7. Rahmat-Samii, Y., Cramer, P., Jr., Woo, K., and Lee, S.W. IEEE Trans. Antennas and Propagat., AP-29, 961—963 (1981).

7. FIGURES

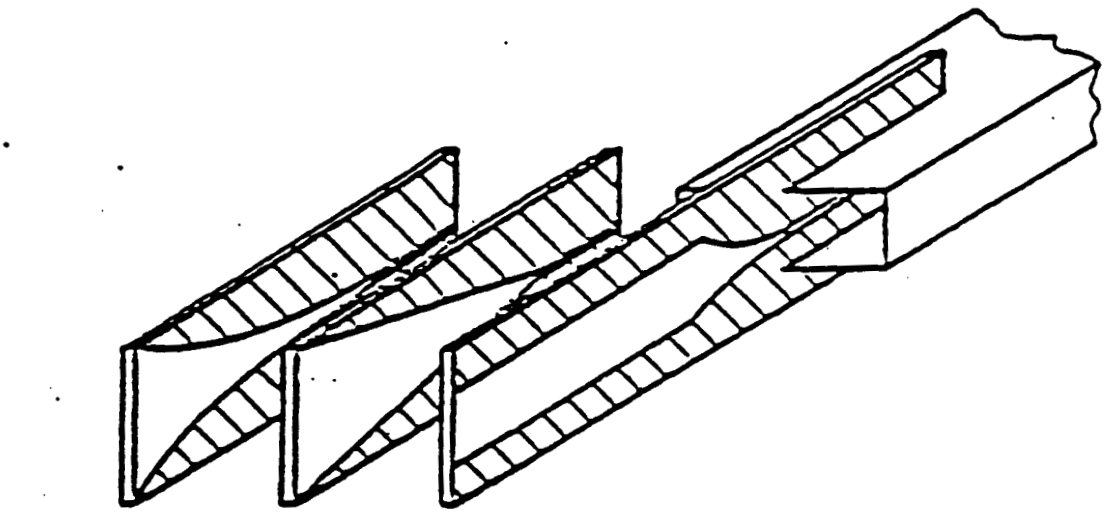

Figure 1. Tapered slot antenna elements with three different shapes

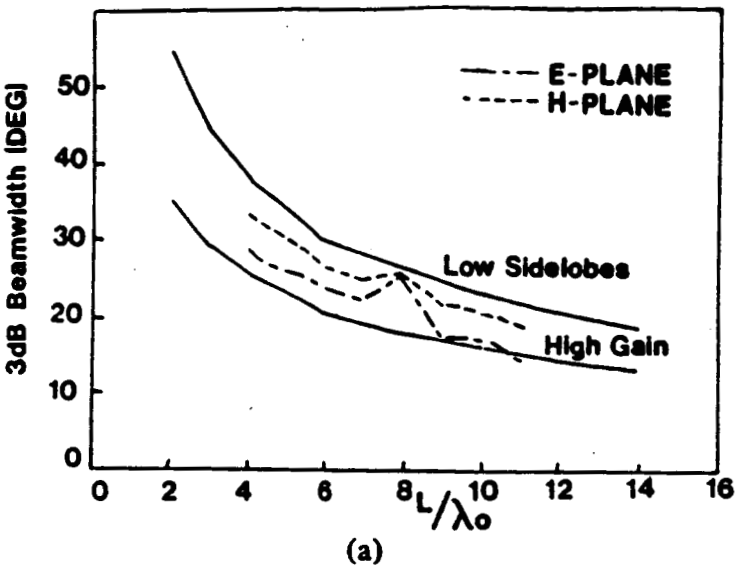

(a)

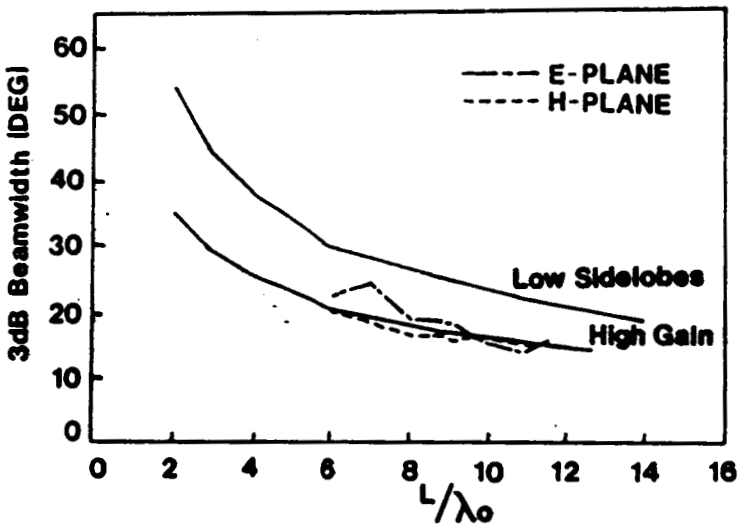

(b)

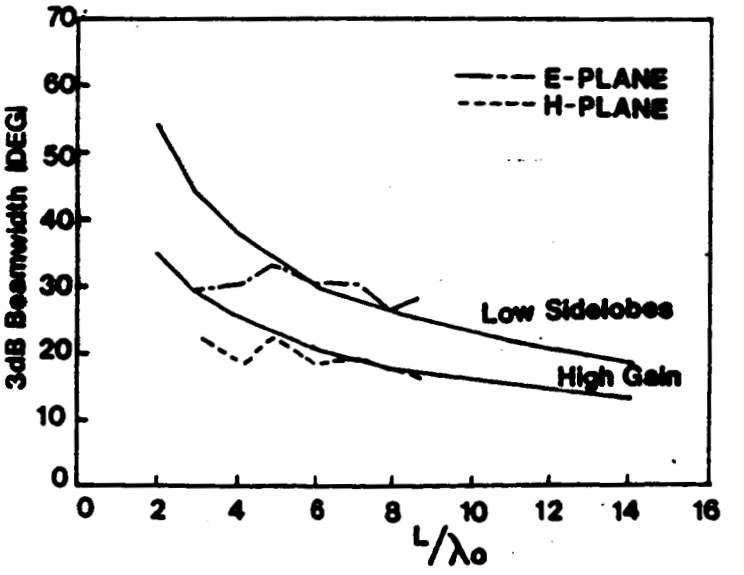

(c)

Figure 2. Beamwidths at 94 GHz for 11.2° LTSA's. (a) On 0.025 mm Kapton. (b) On 0.05 mm Kapton. (c) On 0.076 mm Kapton.

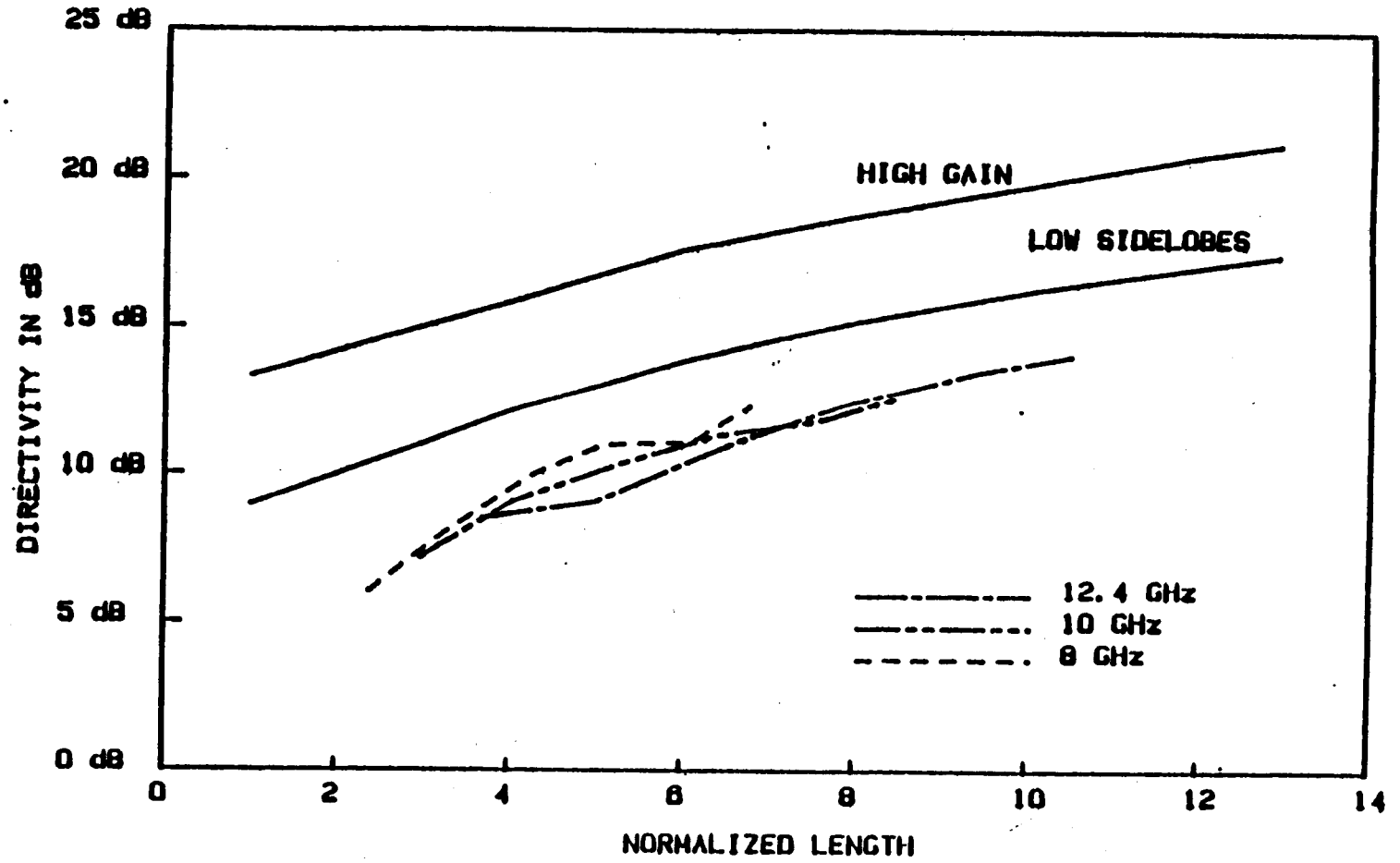

Directivity of LTSA on 0.127 mm thick OAK-605 substrate

Figure 3

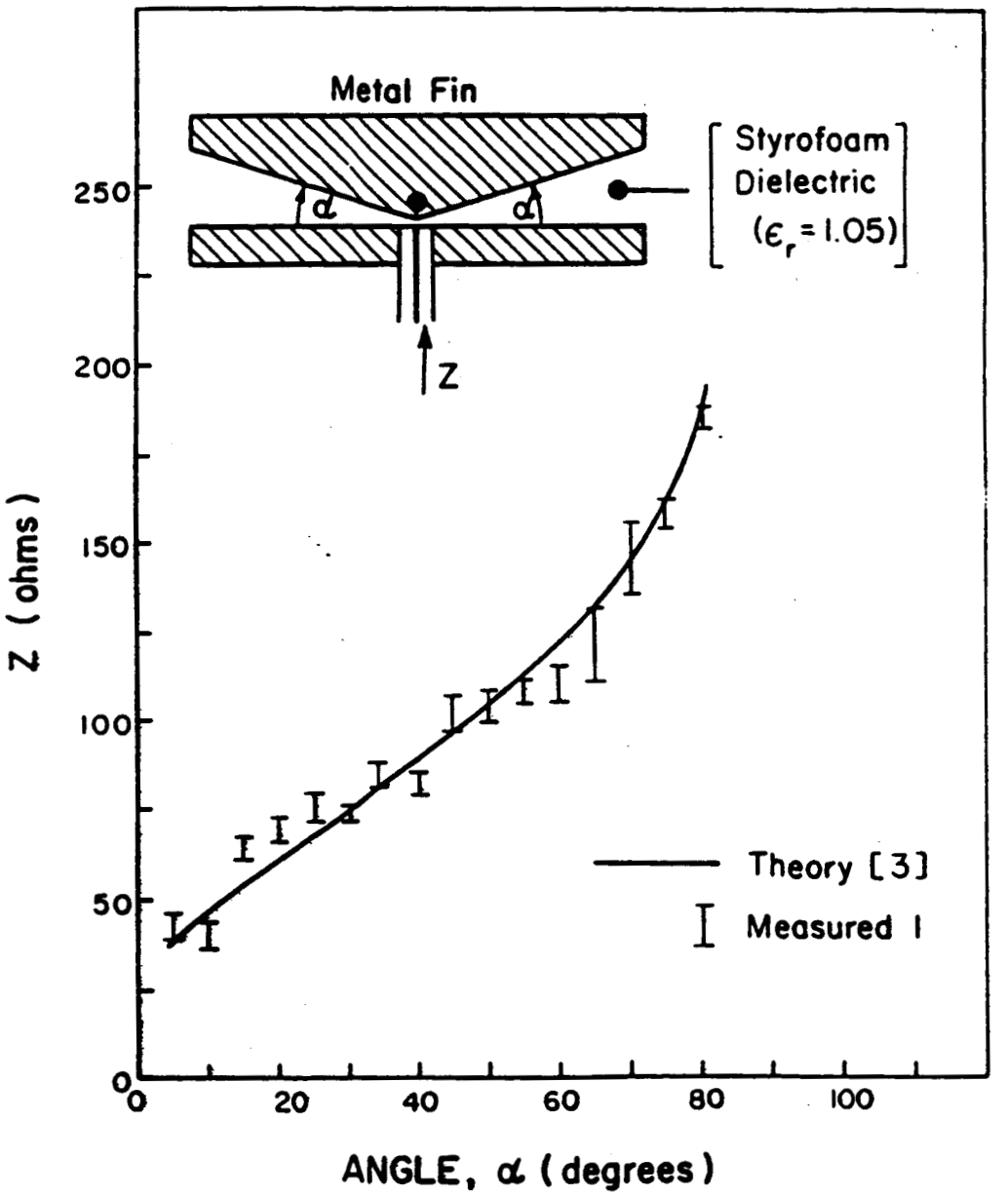

Fig. 4a. Input impedance measured for LTSA pair with styrofoam dielectric, as a function of the opening angle. The geometry is shown in Fig. 3(c).

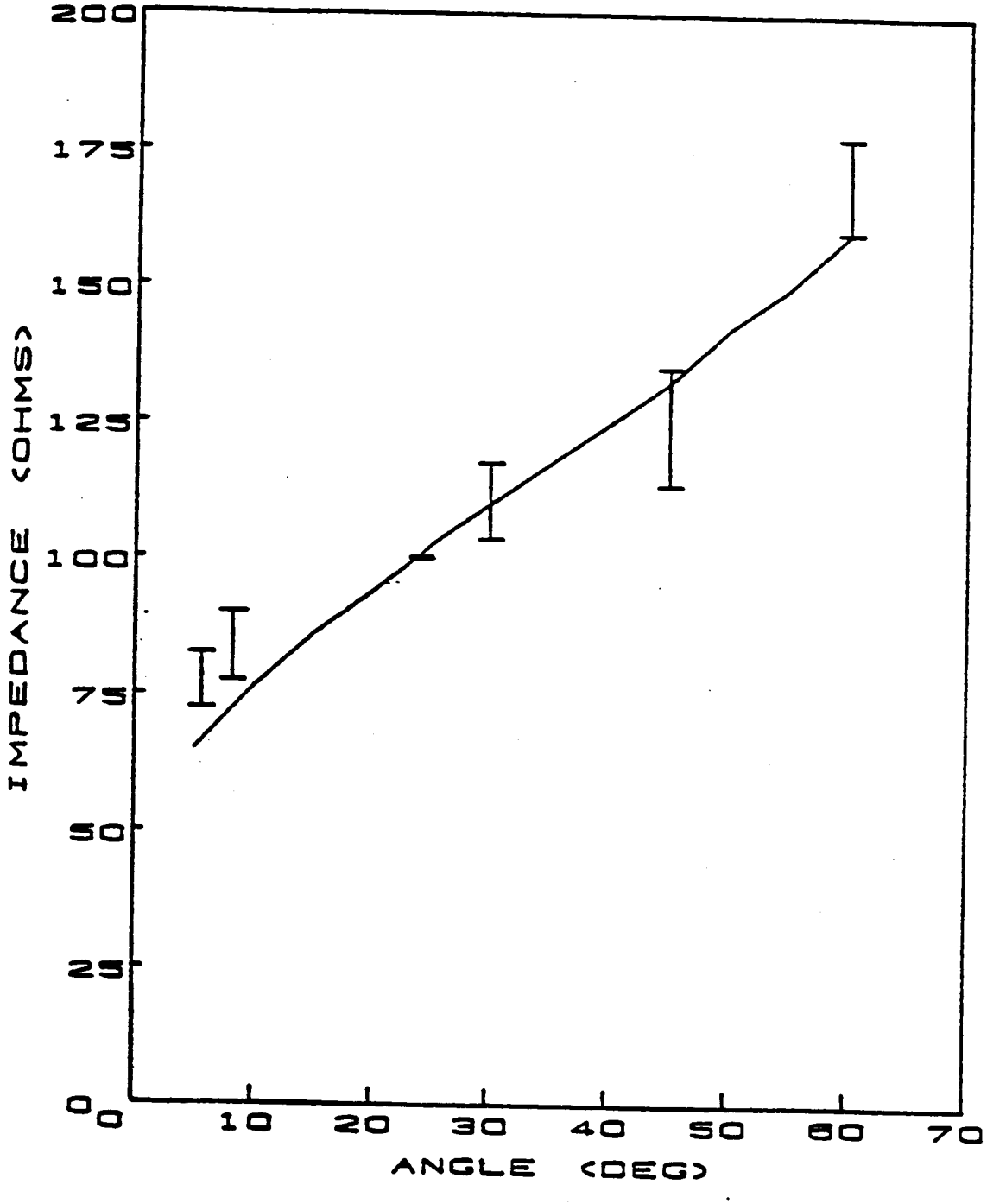

Input impedance of single sided antennas

Figure 4b.

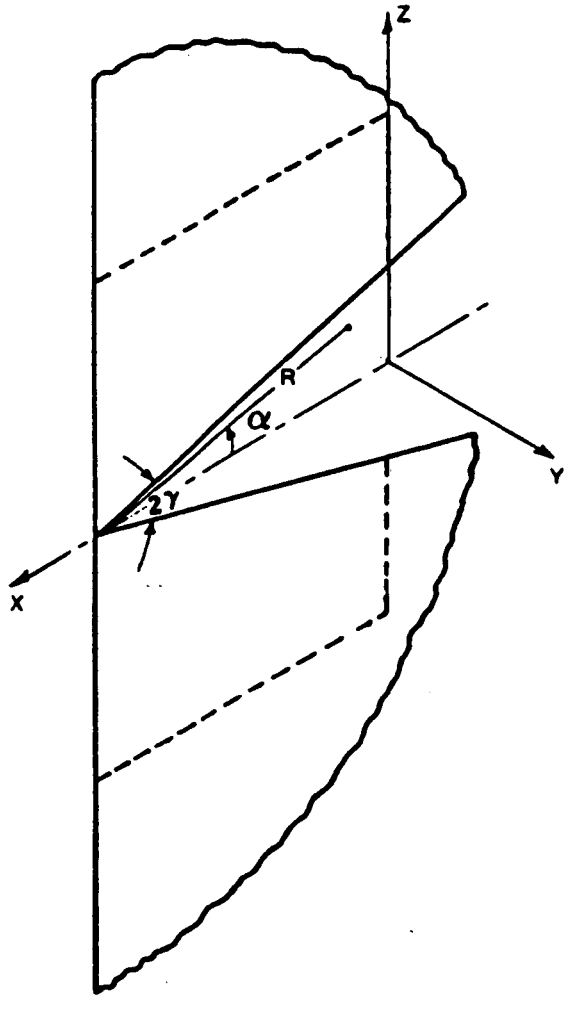

Fig. 5 Geometry of coplanar bifin structure.

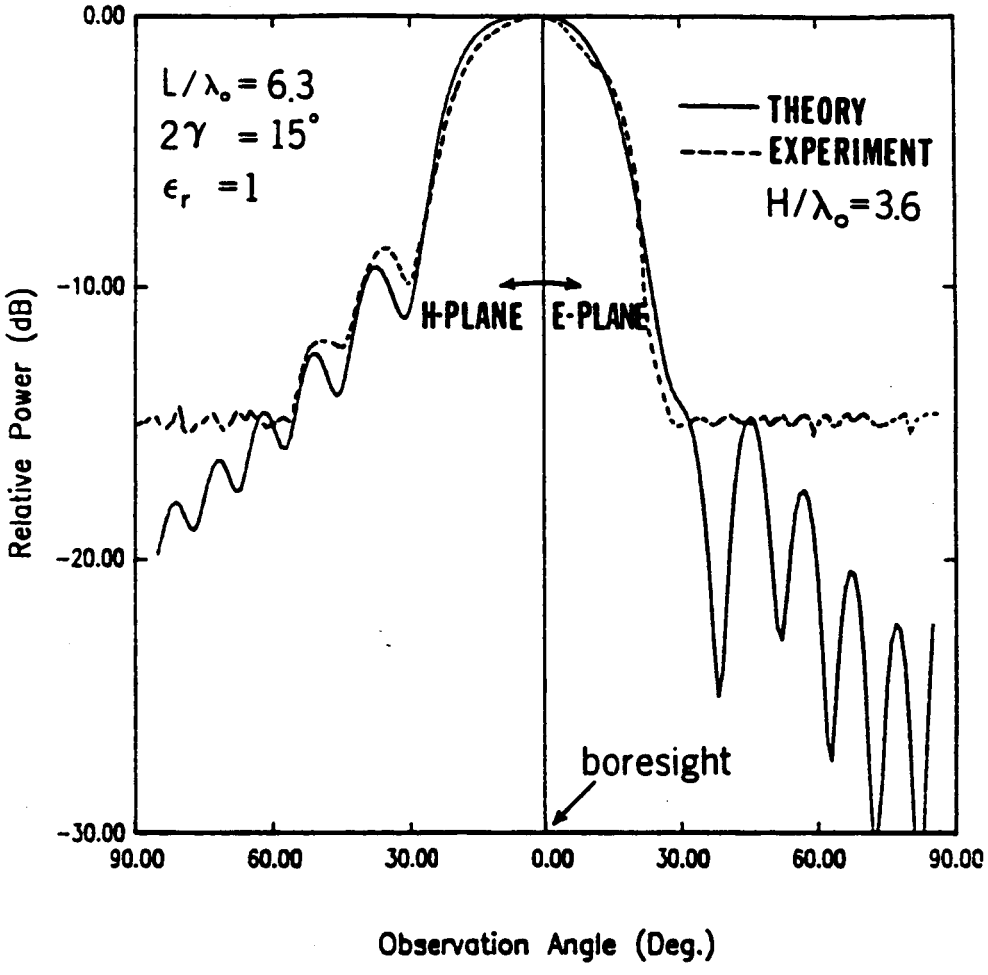

Fig. 6 Radiation pattern of TEM-LTSA.

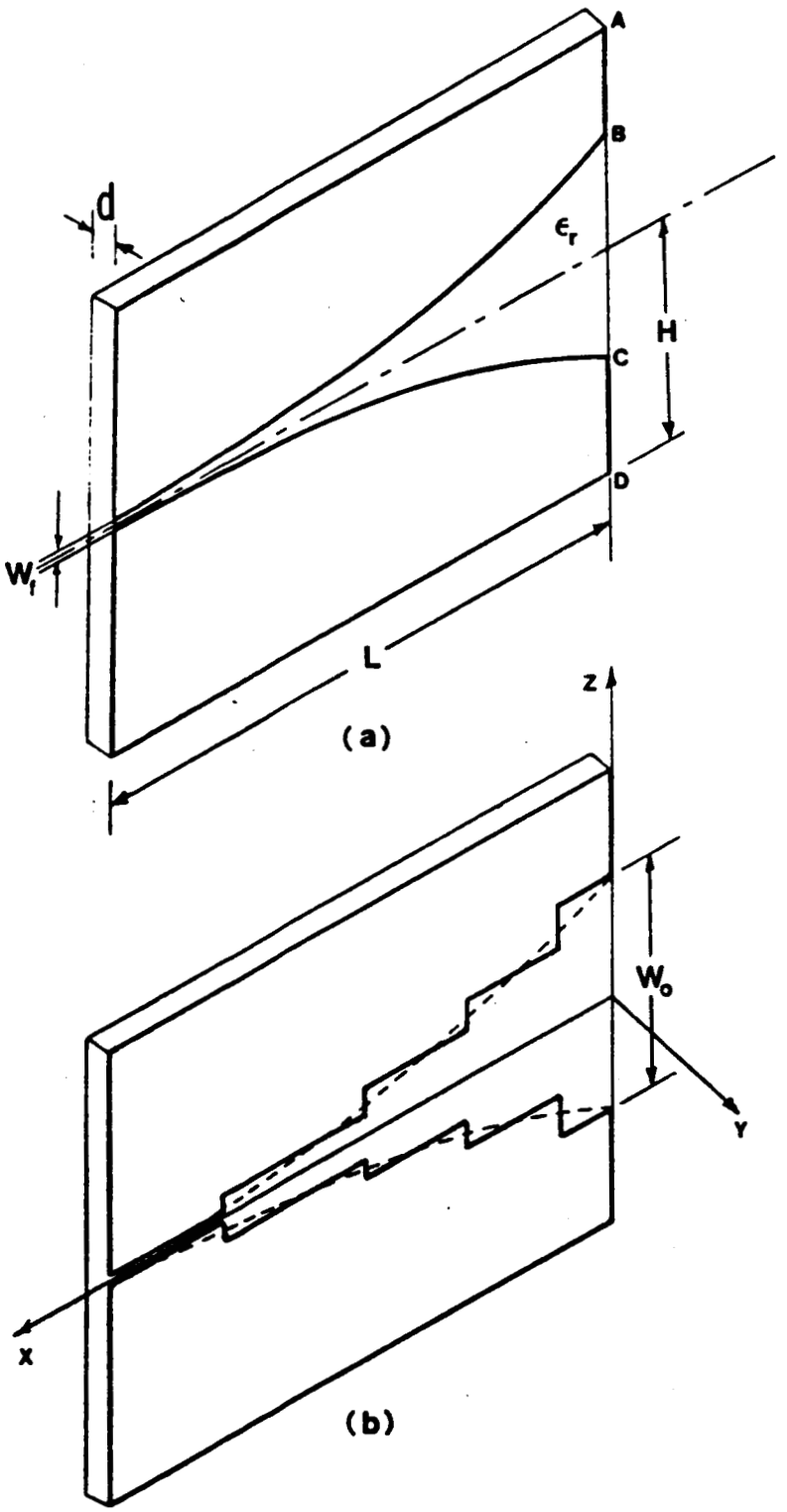

Fig. 7 Geometry of Tapered Slot Antenna. (a) Original problem (b) Stepped approximation.

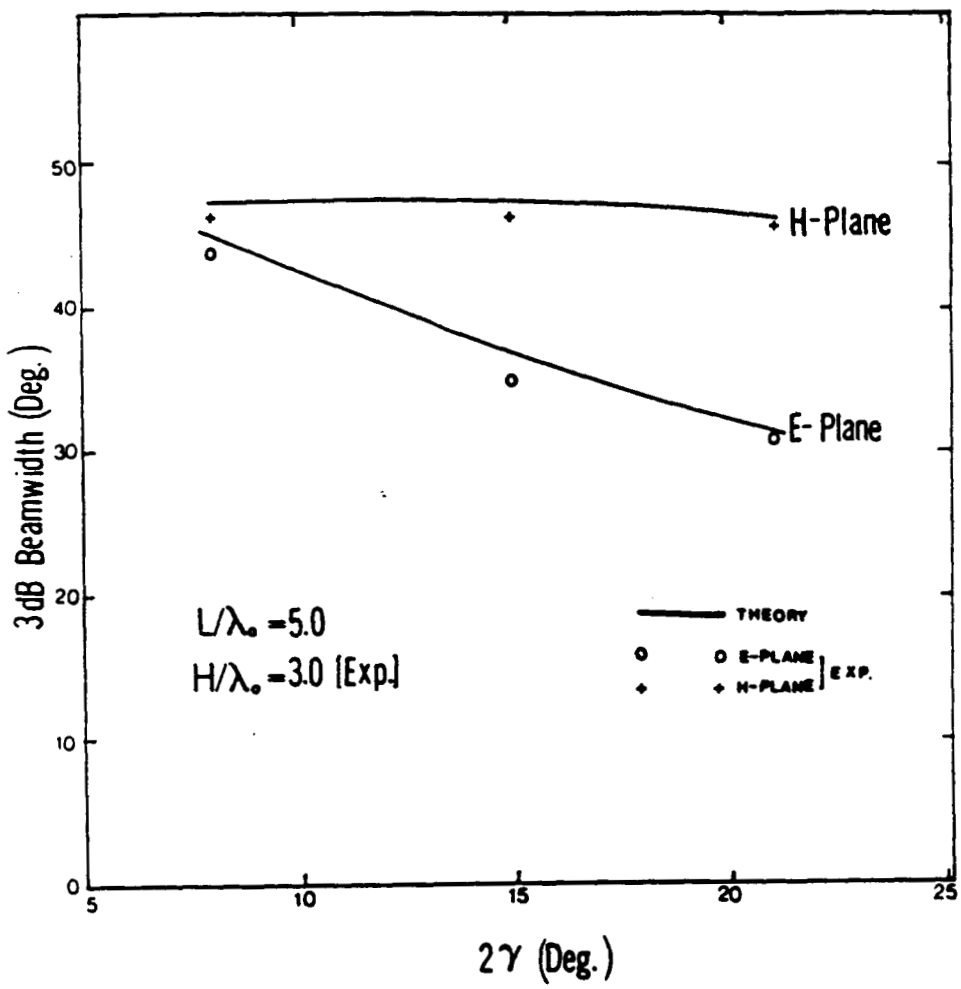

Fig. 8. **Measured and computed beamwidths of TEM–LTSA versus flare-angle.**

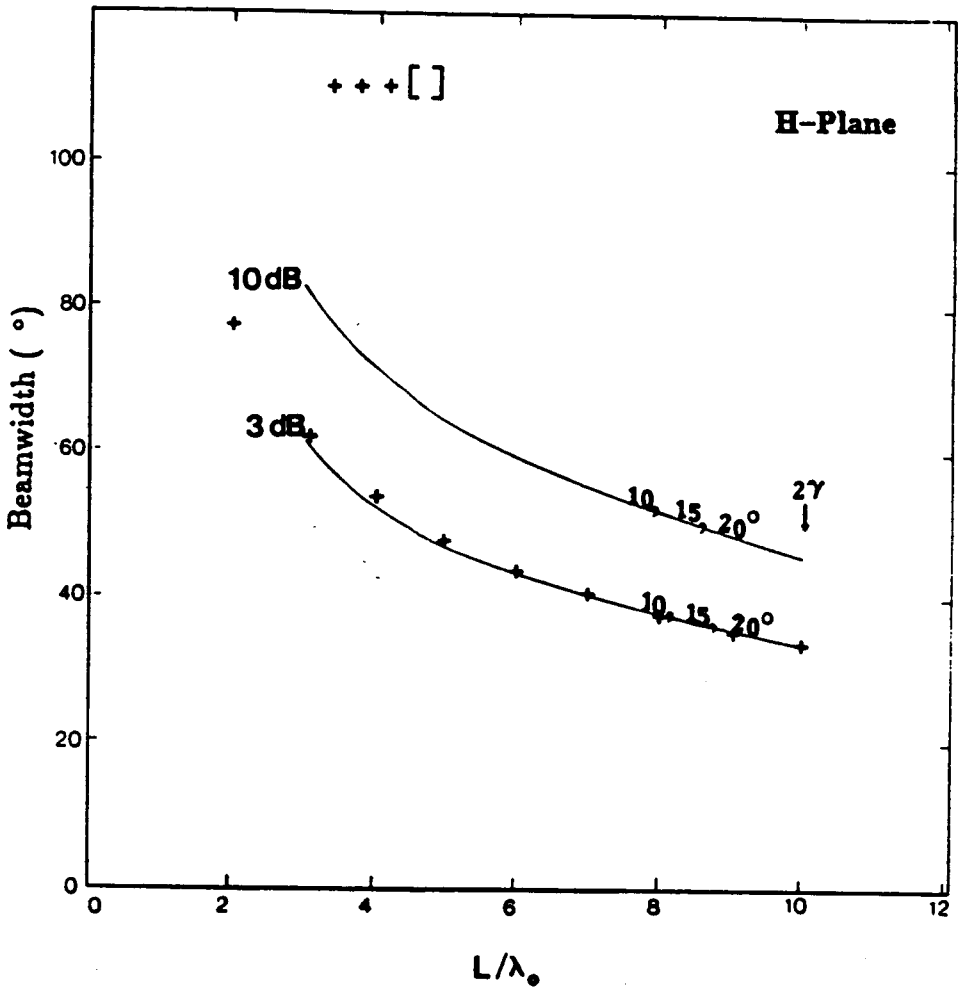

Fig. 9. H-plane beamwidth of TEM-LTSA versus normalized length.

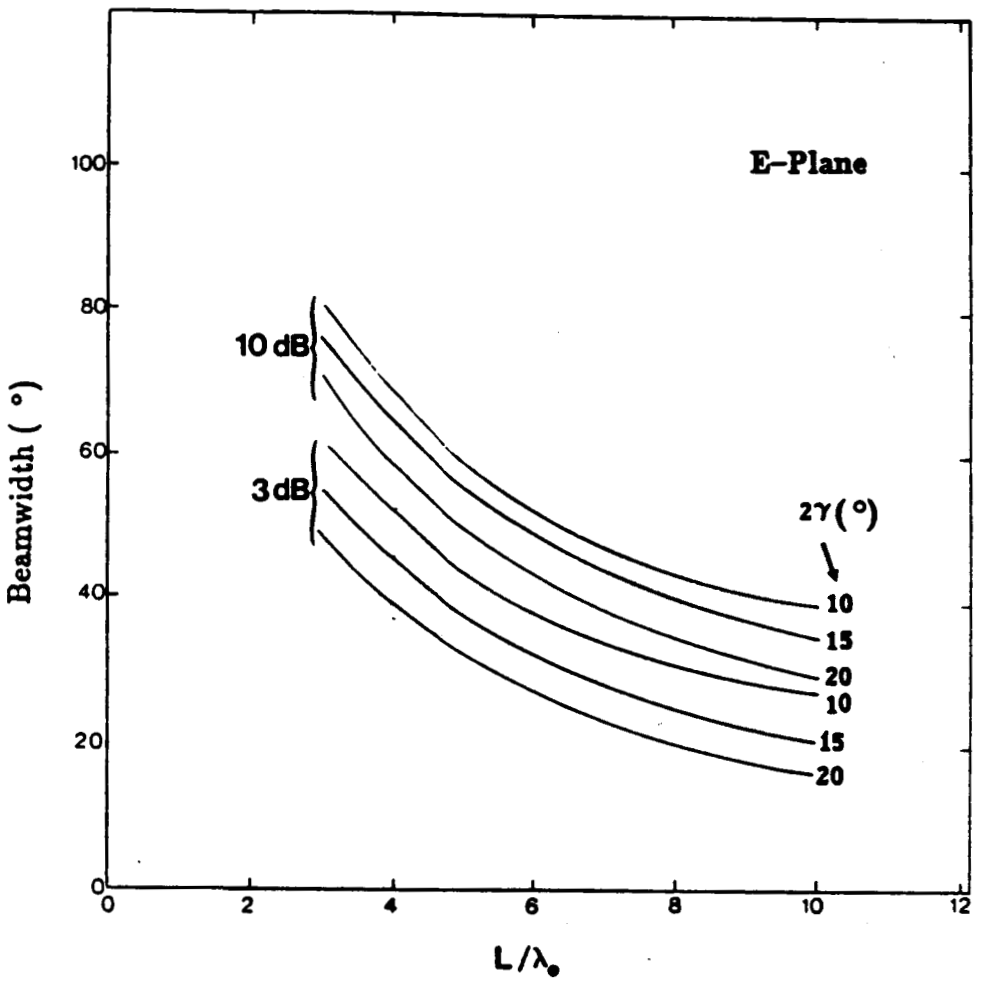

Fig. 10. E-plane beamwidth of TEM–LTSA versus normalized length.

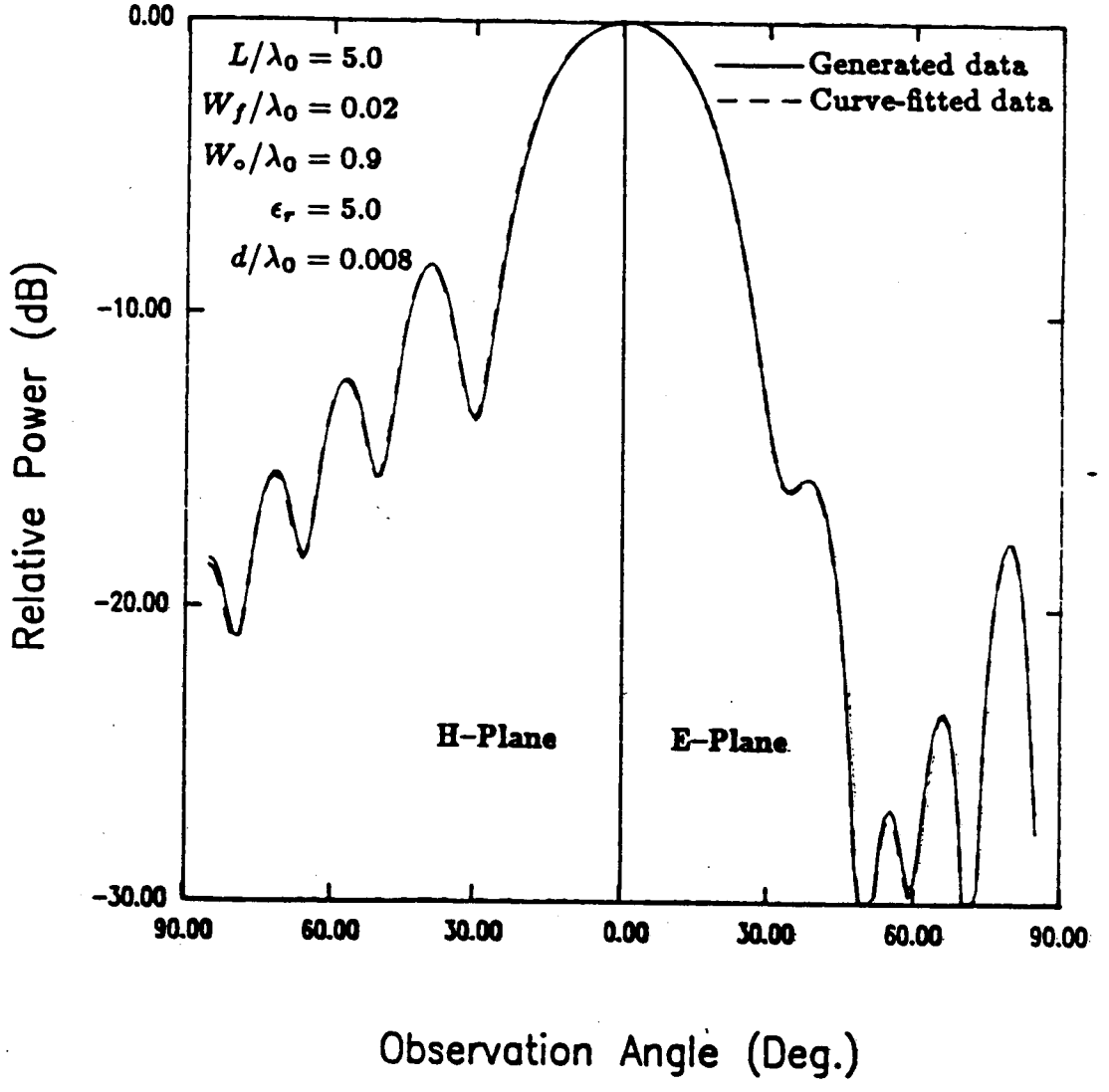

Fig. 12. Computed radiation patterns of CWSA—*generated* and *curve-fitted* slot line data.

PRECEDING PAGE BLANK NOT FILMED

Fig. 11

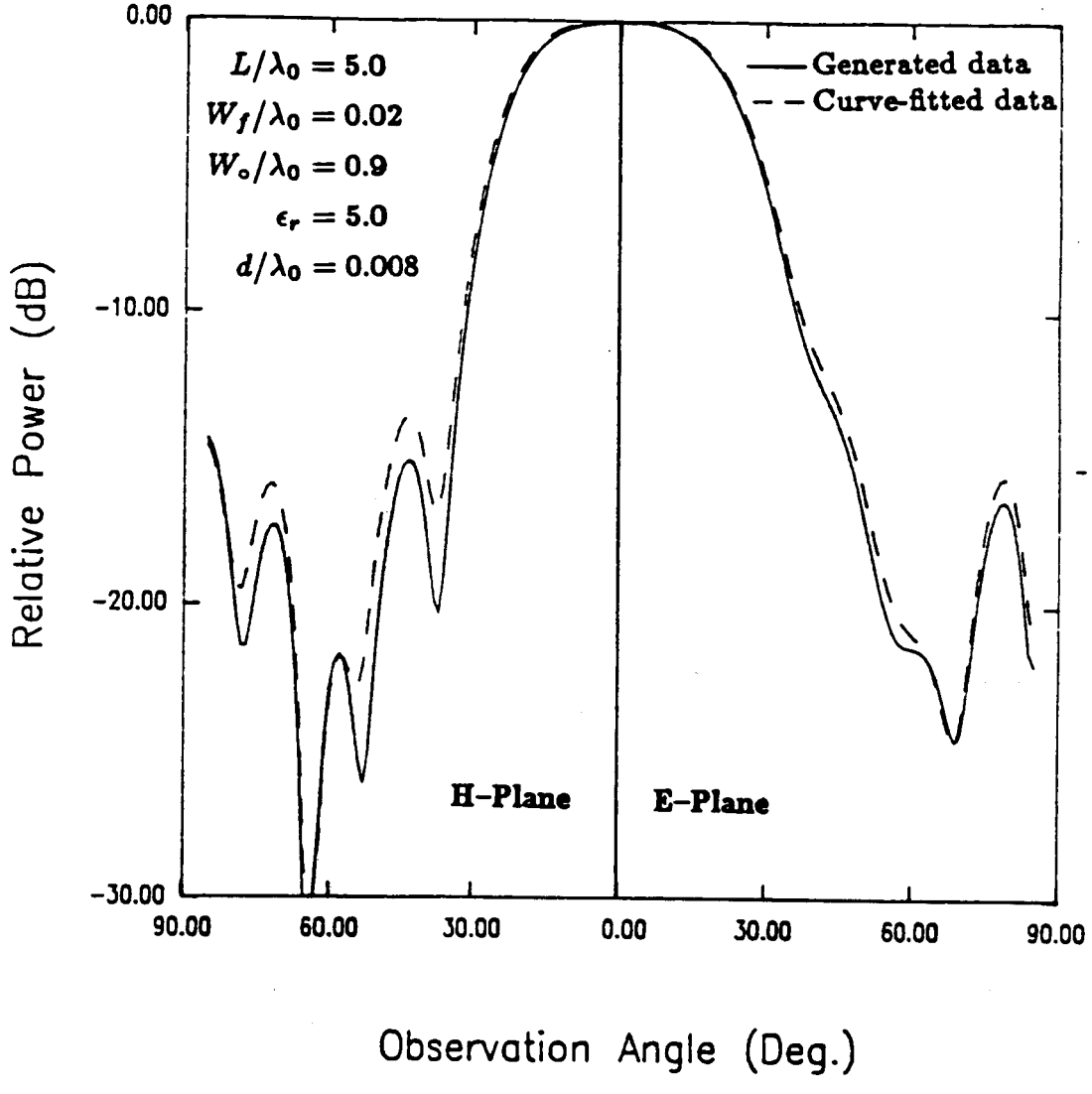

Fig. 13. Computed radiation patterns of Vivaldi—*generated* and *curve-fitted* slot line data.

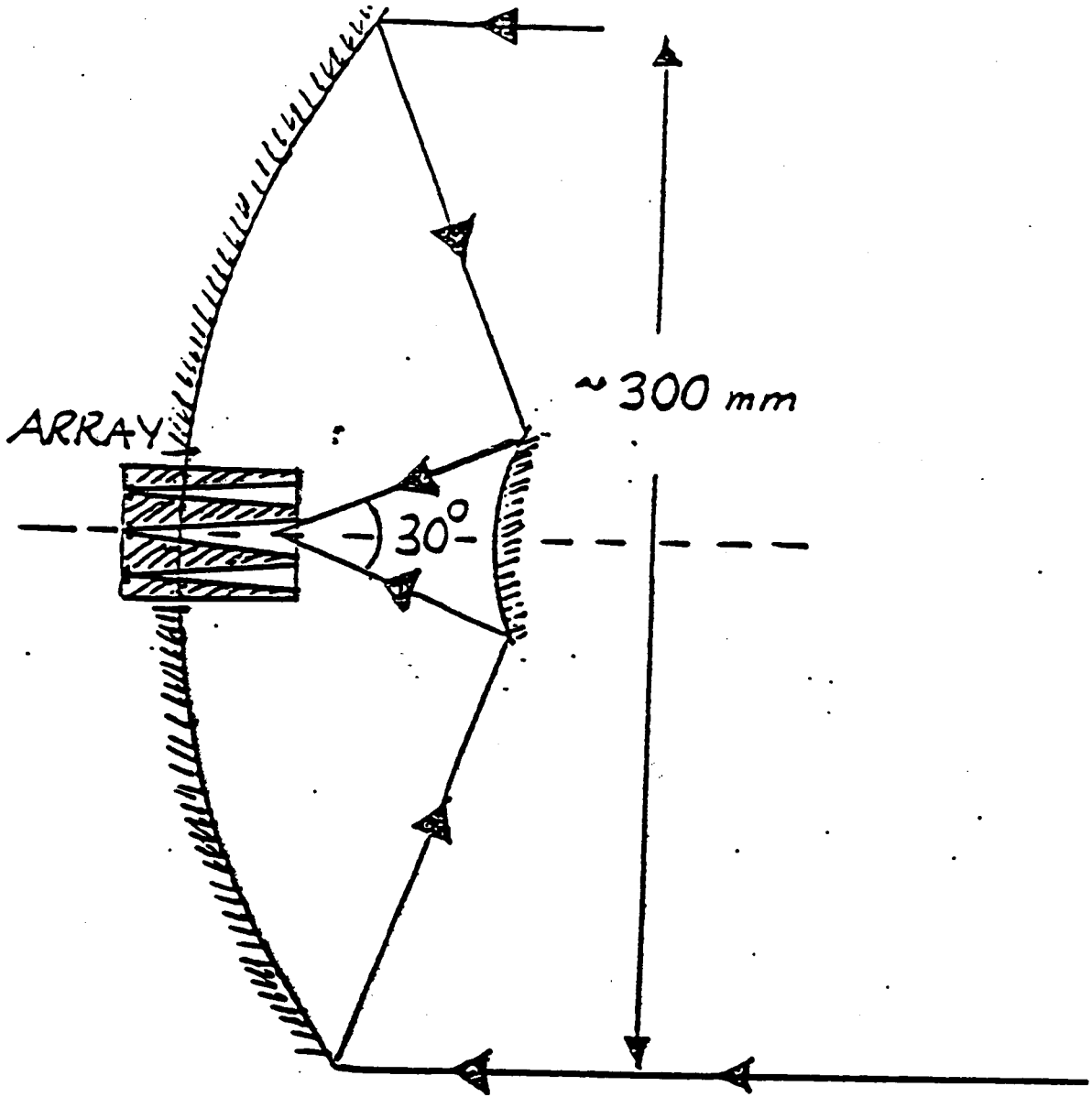

Cassegrain prototype LTSA multi-beam system.

Figure 14.

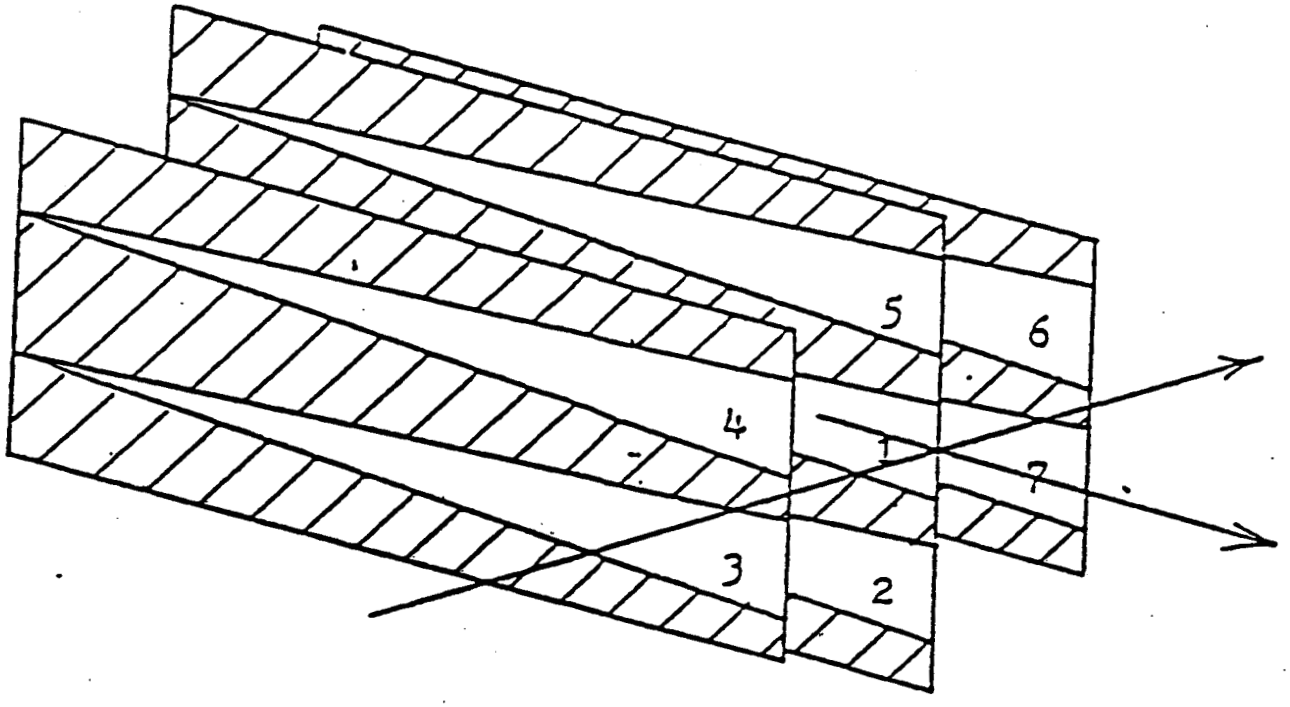

Figure 15. **The seven-element array, used in the Cassegrain prototype multi-beam system.**

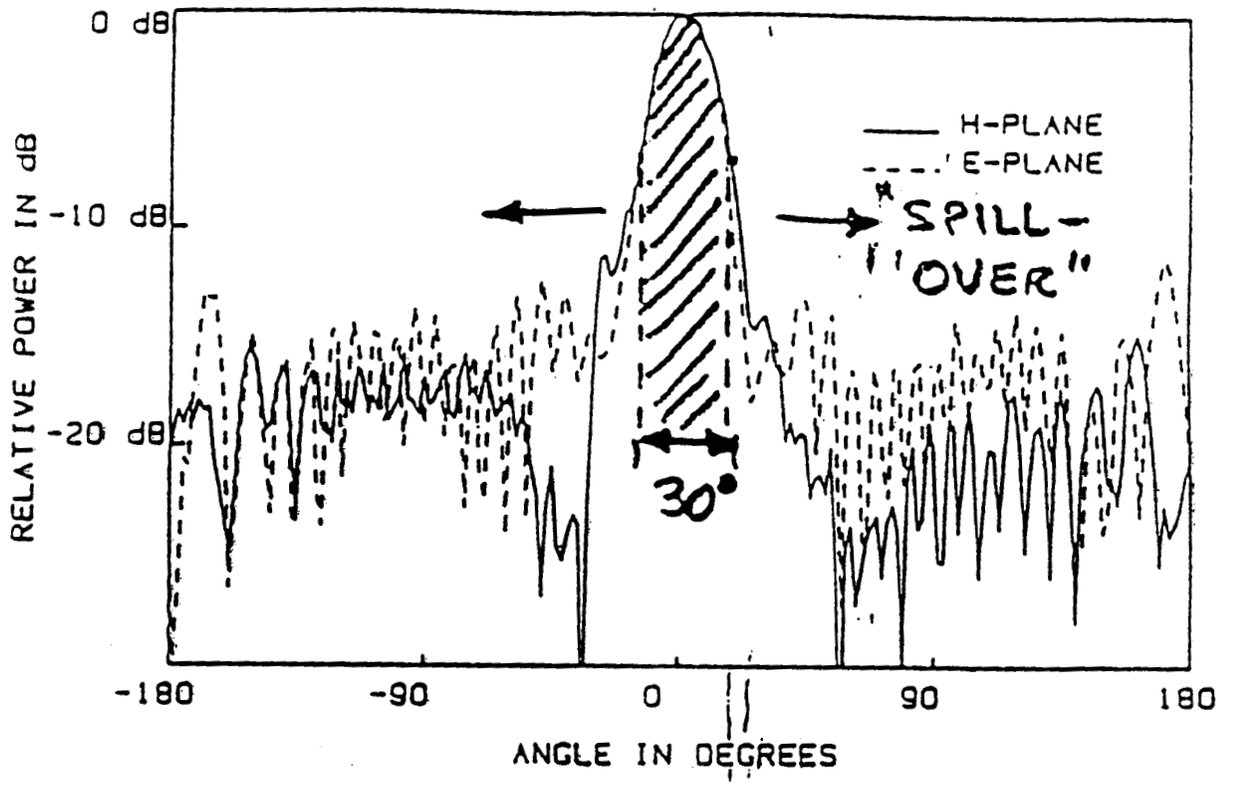

Figure 16. Single-element pattern measured at 94 GHz for LTSA on 1 mil Kapton substrate.

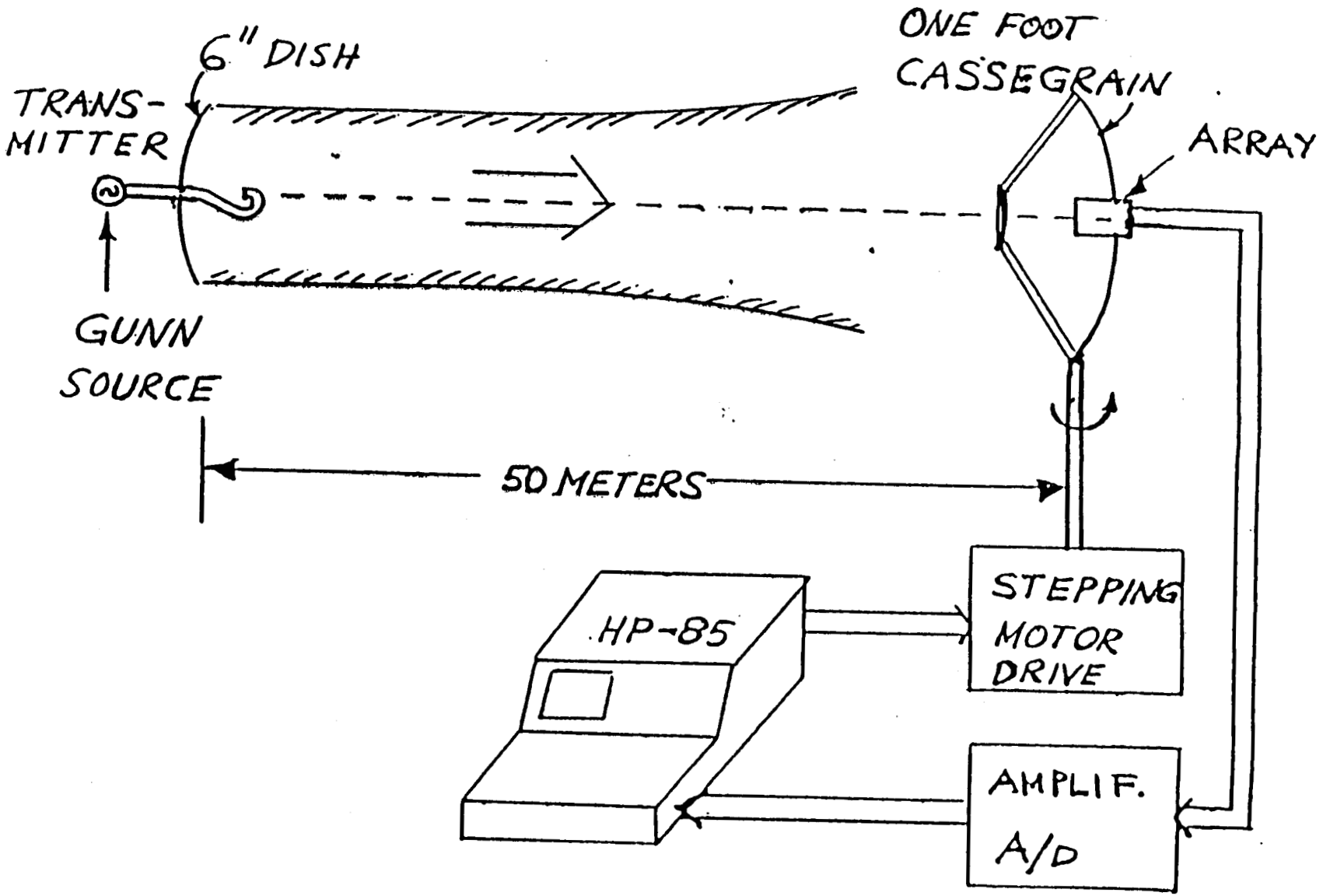

Figure 17. Test range for the Cassegrain prototype multi-beam system.

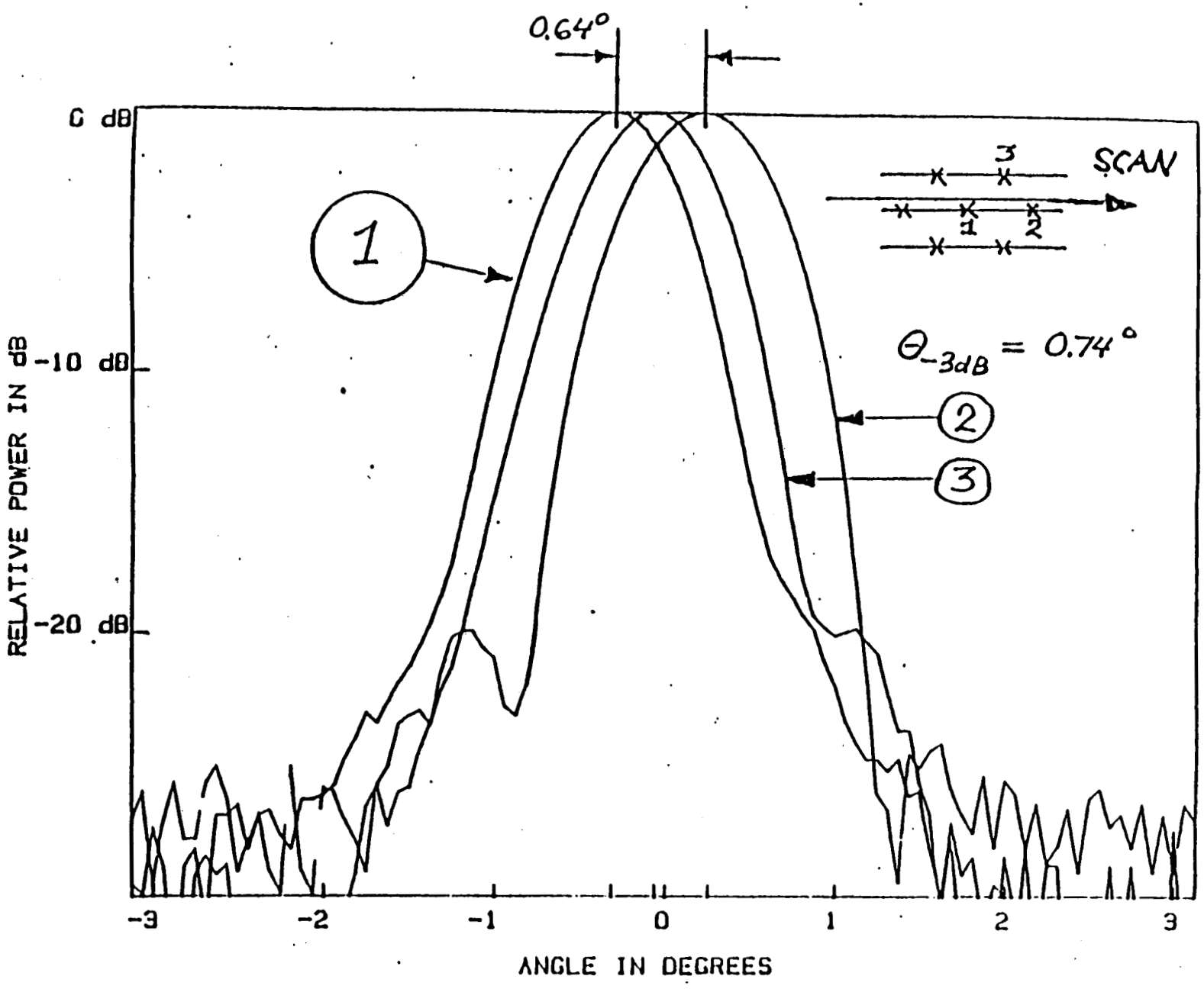

Figure 18. Scans recorded by different beams in the prototype system. Beams are numbered as in Figure 2.2.2 .

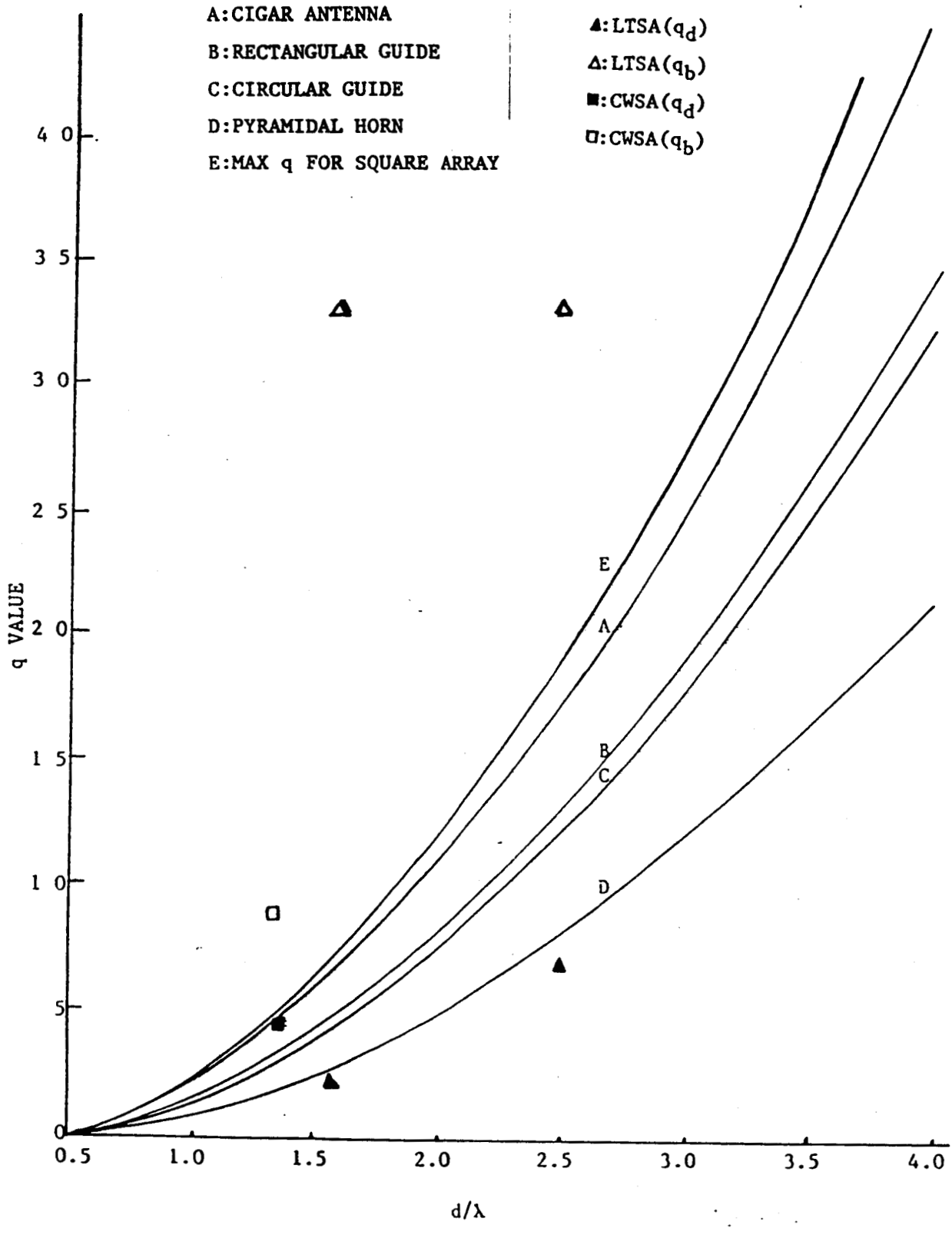

Figure 19. q-value versus d/λ

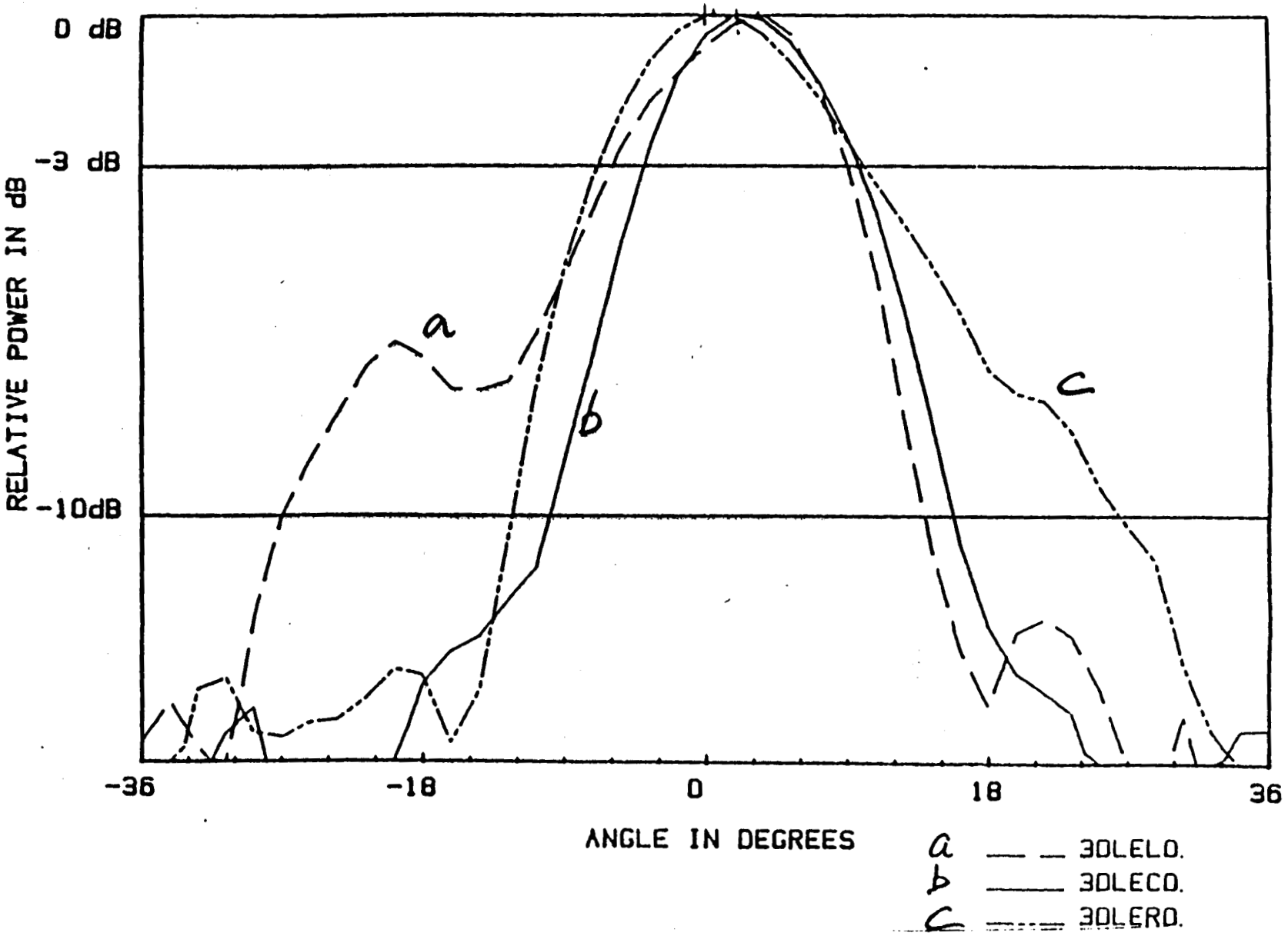

Figure 20. E-plane Element patterns recorded at 94 GHz for a linear array of three LTSA elements with a 3 mm spacing. a) left element b) center element c) right element.

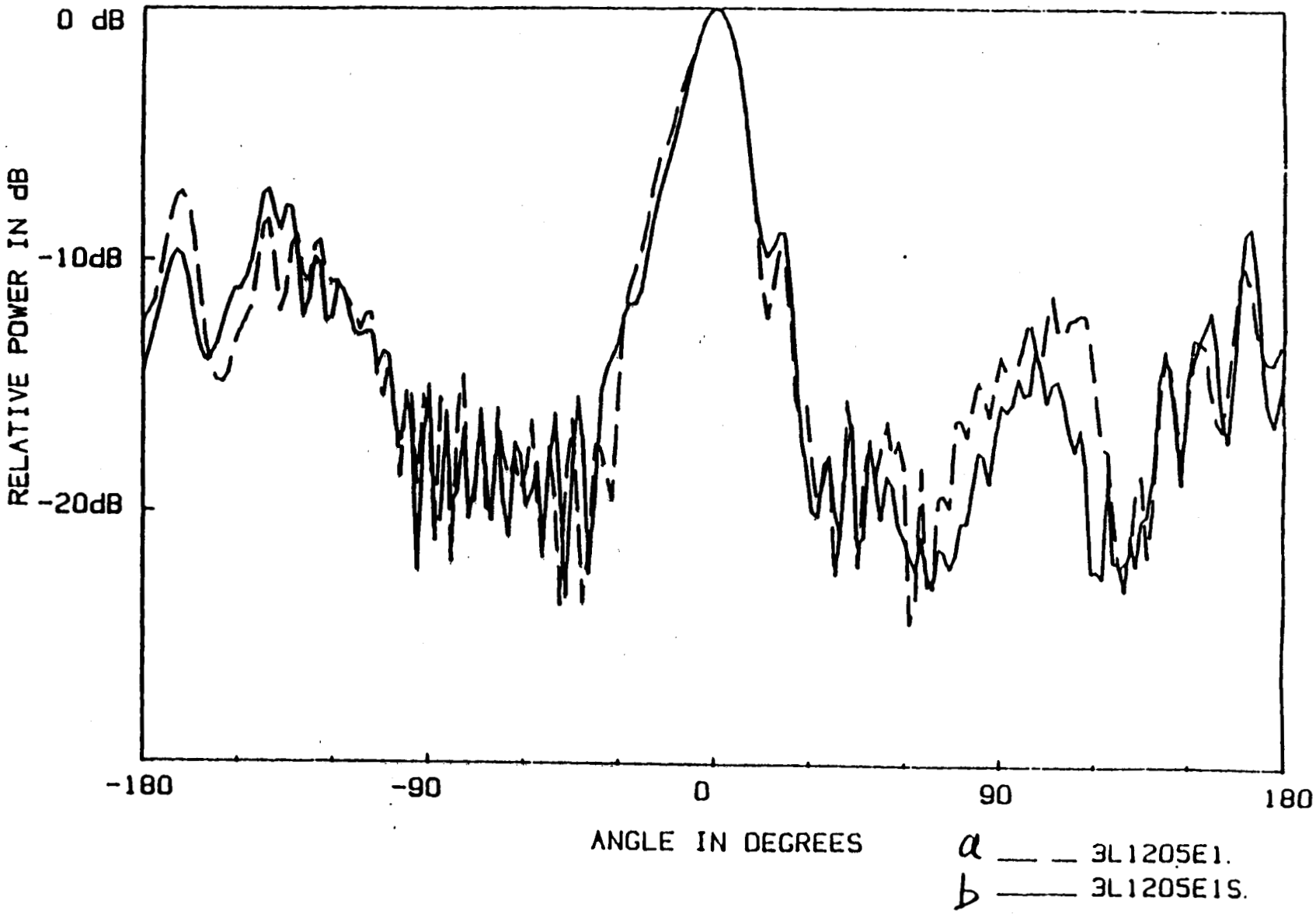

Figure 21 Same array as in Figure 20 . E-plane patterns for edge element when leaving other elements a) open b) shorted.

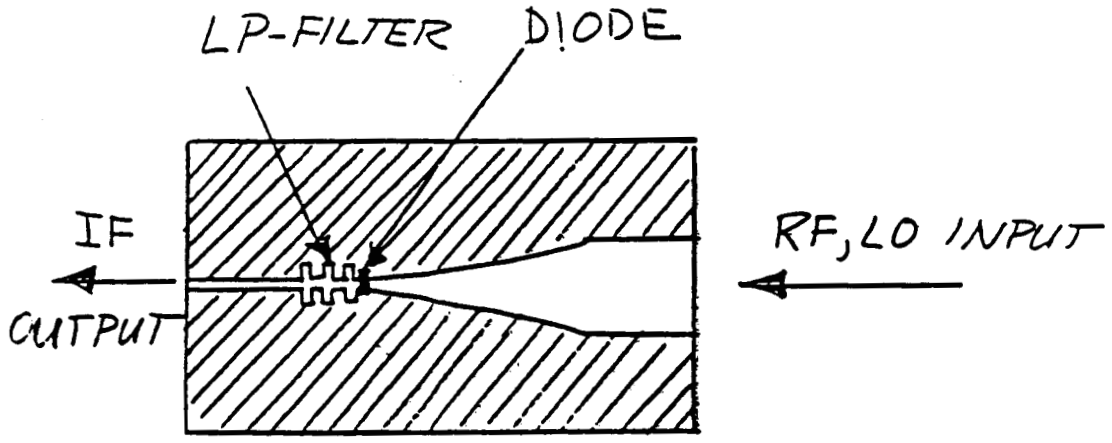

Figure 22. Pattern for 38 GHz mixer, suitable for integration with LTSA element.

8. TABLE

TABLE 1

PATTERN COMPARISON FOR $\epsilon_r = 2.22$ LTSA

	3 dB Beamwidth (°)		10 dB Beamwidth (°)		First SLL (dB)	
	Theory	Measured	Theory	Measured	Theory	Measured
E–plane	39.8	38.3	61.0	57.0	−12.4	−11.5
H–plane	33.7	28.8	50.5	44.4	−10.0	−8.8

$d/\lambda_o = 0.017$, $L/\lambda_o = 4.2$, $2\gamma = 10°$